An Analytical Study of Diffraction by Dielectric Wedges

Zheng Lou
Center for Computational Electromagnetics
Department of Electrical and Computer Engineering
University of Illinois at Urbana-Champaign
Urbana, Illinois 61801-2991

December 19, 2003

1 Introduction

This report describes various asymptotic methods found in literature that have been applied to the analysis of scattering by a dielectric wedge, as the final project for the graduate course *Advanced Electromagnetic Diffraction and Radiation*. For high-frequency methods, such as geometrical theory of diffraction (GTD), it is crucial to find a uniform expression for the diffracted field which compensates for the discontinuity on the optical boundaries caused by the reflected and refracted fields. Unfortunately, it appears that no exact solutions have been found to date for the diffraction by dielectric wedges of arbitrary apex angle and dielectric constant. In the literature, one may observe a dramatic history where claims were made to have solved the problem but turned out immediately afterwards to be erroneous or virtually useless. The solution to the problem, as is different from that of the conducting wedges, is hindered by the fact that wave can penetrate into the dielectric region and one needs to match the boundary conditions on the interfaces between the wedge and the free-space. Since the wavenumbers are different in the two different regions, one-by-one mode matching by analytical methods is almost impossible for arbitrary apex angle. In spite of these difficulties, there have been successful analyses which contribute to the progress in this research topic by pointing out promising directions as well as casting physical insights into the problem. The existing approaches can be characterized by either trying to provide analytical solutions as approximate solution to the original problem under certain assumptions, or trying to solve the problem in an exact sense using combined analytical-numerical methods.

Instead of giving an exhaustive account for the advances made in this field, this report only describes several pronounced attempts, characterized by different methods. These methods include old-fashioned modal analysis [1], null-field method [2], physical optics (PO) method [3], and the newly-developed integral-transform methods [5]. A general review of the dielectric wedge diffraction problem is available in G. James's book [6], which is the starting point of this project. Computer codes are also implemented for some of the schemes for better understanding of the subject.

2 General Problem Description

The geometry and the related symbols are defined in Fig. 1. The Ω_1 and Ω_2 denote the dielectric and free-space regions, respectively. The Γ_1 and Γ_2 denote the two edges of the wedge. The symmetry axis of the wedge coincides with the x-axis and the half angle of wedge apex is denoted by χ. The wedge is illuminated by either a plane wave from outside with incident angle ϕ_0, or by a line source positioned inside or outside the wedge.

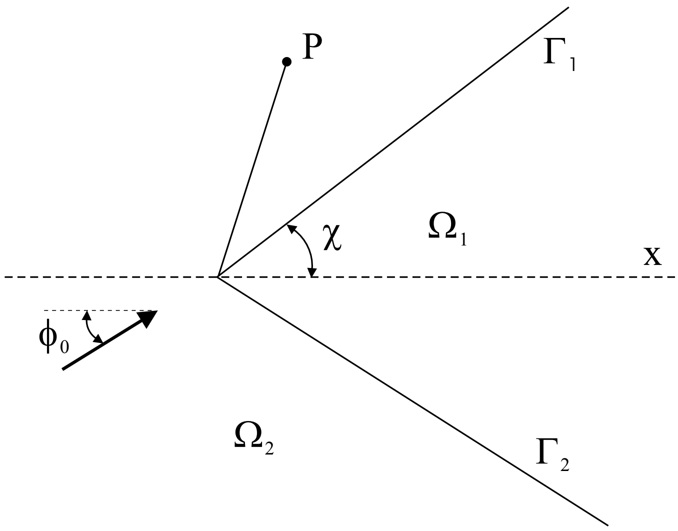

Figure 1: Geometry of dielectric wedge with plane wave incidence.

3 Mode Matching

In [1], the traditional modal analysis is applied to the wedge diffraction problem. The key point is to choose appropriate wavefunctions to represent the exact field, especially near the apex of the wedge.

The wave equations for the longitudinal field component in Ω_1 and Ω_2 are

$$\nabla^2\Phi + \nu^2 k^2 \Phi = 0 \qquad \text{in} \quad \Omega_1 \tag{1}$$

$$\nabla^2\Psi + k^2 \Psi = 0 \qquad \text{in} \quad \Omega_2 \tag{2}$$

and the boundary conditions to be satisfied are

$$\Phi = \Psi \qquad \text{on} \quad \Gamma_1, \quad \Gamma_2. \tag{3}$$

$$\partial\Phi/\partial\phi = \partial\Psi/\partial\phi \qquad \text{on} \quad \Gamma_1, \quad \Gamma_2 \tag{4}$$

To simplify the analysis, a line source is placed on the symmetry axis of the wedge, say $Q(\rho_0, 0)$, generating out-going cylindrical wave represented by Hankel function of second kind. Accordingly, we can separate Φ into the field produced by the source Φ^e and the reflected (refracted) field Φ^r so that $\Phi = \Phi^e + \Phi^r$. If we are only interested in the $\rho < \rho_0$ region, Φ^e can be represented by the bessel functions

$$\Phi^e(\rho, \phi) = \sum_{n=1}^{\infty} a_n \Phi_n^e(\rho, \phi) \tag{5}$$

$$\Phi_n^e(\rho, \phi) = J_n(\nu k\rho)\sin(n|\phi|), \quad \rho < \rho_0 \tag{6}$$

The wavefunctions (expansion functions) for Φ^r and Ψ need to be determined. One may still use bessel functions, but difficulty arises when one tries to match the boundary condition for bessel functions with different argument ($k\rho$ and $\nu k\rho$ respectively). This difficulty can be ameliorated by using the following equality:

$$J_\alpha(\nu\zeta) = \sum_{n=0}^{\infty} F_n(\alpha, \nu) J_{\alpha+2n}(\zeta), \quad \alpha \neq I_- \tag{7}$$

where

$$F_n(\alpha, \nu) = (-1)^n \nu^{\alpha+2n}(\alpha + 2n) \sum_{m=1}^{\infty} \frac{(-1)^m \nu^{-2m}\Gamma(\alpha + 2n - m)}{m!(n-m)!\Gamma(\alpha + n - m + 1)}, \tag{8}$$

where Γ is the gamma function. Equation (7) and (8) are the crux of the proposed method. By inspecting (7) and (8) and invoking the symmetry of the geometry, one may find the appropriate forms of Φ_n^r and Ψ_n as

$$\Phi_n^r(\rho, \phi) = \sum_{m=-m1}^{\infty} A_m J_{n+2m}(\nu k\rho)\cos((n + 2m)\phi); \tag{9}$$

$$\Psi_n(\rho, \phi) = \sum_{m=-m2}^{\infty} B_m J_{n+2m}(k\rho)\cos((n + 2m)(\pi - \phi)); \tag{10}$$

As a result, the wavefunction for the total field inside wedge region becomes

$$\begin{aligned}\Phi_n(\rho, \phi) = & \sum_{m=0}^{\infty} F_m(n, \nu) J_{n+2m}(k\rho)\sin(n|\phi|) \\ & + \sum_{m=-m1}^{\infty}\sum_{q=0}^{\infty} A_m F_q(n + 2m, \nu) J_{n+2m+2q}(k\rho)\cos((n + 2m)\phi).\end{aligned} \tag{11}$$

Now, the arguments of the bessel functions in (10) and (11) become identical, which significantly simplifies the modal analysis. The coefficients A_m and B_m

can be therefore determined by substituting (10) and (11) into the boundary conditions (3) and (4). This will result in a coupled series-equation regarding A_m and B_m which can be solved iteratively [1].

The method has the advantage that the formulae used to find the expansion coefficients are computationally inexpensive. Moreover, the wavefunctions used to expand the fields have clear physical meaning and are capable of modeling the field in the vicinity of the apex of a dielectric wedge.

4 Null-Field Method

In [2], a similar scheme is employed in the analysis of dielectric wedge. Attention is paid to the field behavior near the apex of the wedge. In the context of GTD, it is conventional to split the total field as

$$u(\rho, \phi) = u_0(\rho, \phi) + u_r(\rho, \phi) + u_d(\rho, \phi) \tag{12}$$

where r stands for the reflected field outside the wedge and the refracted field inside the wedge and d stands for the diffracted field. For plane wave incidence,

$$u_0(\rho, \phi) = \exp[-jk\rho\cos(\phi + \phi_0)]. \tag{13}$$

Given (13), the reflected and refracted wave can be written accordingly , making use of Fresnel reflection and transmission coefficients for infinite planar interfaces. For an arbitrary observation point P outside the wedge, the following integral equation is valid:

$$\begin{aligned} h(P) &= -\int_{\Gamma_1,\Gamma_2} [G_0(P,Q)\partial u(Q) - u(Q)\partial G_0(P,Q)]\, dr' \\ &= -u_0(\rho,\phi) \qquad\qquad \text{in} \quad \Omega_1 \\ &= u_r(\rho,\phi) + u_d(\rho,\phi) \qquad \text{in} \quad \Omega_2 \end{aligned} \tag{14}$$

where Q is the observation point on one of the two edges of the wedge and $G_0(P,Q)$ is the 2D Green's function for free-space. The integral equation can be derived from equivalence principle by relating $u(\rho, \phi)$ to the equivalent magnetic current and $\partial u(\rho, \phi)$ to the equivalent electric current on Γ_1 and Γ_2. The effect of these equivalent currents is to extinguish the incident field inside the wedge region, thus producing zero total field (null-field) in Ω_1.

To solve the integral equation (14), it is convenient to first expand the field with wavefunctions. Using wave transformation, u_0 can be written as

$$u_0(\rho, \phi) = \sum_{n=0}^{\infty} \epsilon_n (-j)^n J_n(k\rho)\cos[n(\phi + \phi_0)] \tag{15}$$

where $\epsilon_n = 1$ for $n = 0$ and $\epsilon_n = 2$ for $n > 0$. The appropriate form for u_d is unknown, but it is assumed that u_d also takes similar form as u_0 for observation point within an adequate distance from the apex. That is

$$u_(\rho, \phi) = \sum_{n=0}^{\infty} A_n^{(m)} J_n(k\rho)\cos[n\phi + \Phi_n^{(m)}] \qquad \phi_{m1} < \phi < \phi_{m2} \tag{16}$$

where m denotes the angular sectors defined by the optical boundaries, which lie on $\phi = \phi_{m1}$ and $\phi = \phi_{m2}$ for sector m. The assumption is supported by the fact that the total field should be analytic at the apex of the wedge and that the diffracted field should be discontinuous on the optical boundaries. The $A_n^{(m)}$ and the $\Phi_n^{(m)}$ are unknown constants to be determined from the continuity conditions applied on the optical boundaries.

Substituting (15) and (16) into (14) and equating the coefficients of each $J_n(k\rho)$ terms, one is able to obtain

$$\epsilon_n(-j)^n \cos[n(\phi + \phi_0)] = -\sum_{m=0}^{\infty} B_{n,m} \cos(m\phi + \Psi_{n,m}). \tag{17}$$

Equation (17) constitutes, after truncation, a linear system of equations that can be used to solve the unknown coefficients. After $B_{n,m}$ and $\Psi_{n,m}$ are solved numerically, coefficients $A_n^{(m)}$ and $\Phi_n^{(m)}$ can be found and u_d can be recovered. The relation between $A_n^{(m)}$ and $B_{n,m}$, $\Phi_n^{(m)}$ and $\Psi_{n,m}$ can be found through substituting corresponding expressions into (14). Note that the u_d found by (16) is only valid for near field. However, the far field pattern can be readily calculated form the standard asymptotic evaluation of (14), with the total field replaced by the series representation. Hence, a global solution can be obtained.

It is also noteworthy that when reflected or refracted wave impinges upon the face opposite that at which reflection or refraction occurs, multiple reflection or refraction will takes place. In these cases, it is crucial to separate the multi-reflected or multi-refracted wave from the diffracted wave properly to obtain satisfactory numerical convergence.

5 Physical Optics Solution

Similar to the null-field method, the method described in [3] starts with the integral equation (14). Let $A(\alpha, \beta)$ denote the Fourier transform of the total field $u(x, y)$ inside the wedge. A spectral-domain expression for the integral equation is

$$u(x, y) = F^{-1}\{A(\alpha, \beta)\} \tag{18}$$

$$\begin{aligned} A(\alpha, \beta) = & -\frac{1}{\alpha^2 + \beta^2 - k_d^2} \\ & \cdot\{\int_0^{\infty} [-j\beta u(x, 0) + \partial u(x, 0)/\partial y]\, e^{j\alpha x} \\ & + \int_0^{\infty} [-j\beta u(0, y) + \partial u(0, y)/\partial x]\, e^{j\beta y}\} \end{aligned} \tag{19}$$

The boundary field $u(x, 0)$ and $u(0, y)$ may be obtained by assuming wedge interfaces are infinite planes and applying Fresnel reflection and transmission formulae. After substituting the PO approximation of the boundary fields into (19), $A(\alpha,\beta)$ can be approximated as

$$A_p(\alpha,\beta) = -\frac{1}{\alpha^2+\beta^2-k_d^2}\{T_x\frac{\beta+k_v\sqrt{\epsilon-\cos^2\phi_0}}{\alpha-k_v\cos\phi_0}+T_y\frac{\alpha+k_v\sqrt{\epsilon-\sin^2\phi_0}}{\beta-k_v\sin\phi_0}\} \tag{20}$$

where k_v and k_d are the wavenumbers in the free-space and dielectric, respectively. The total field can be obtained by applying inverse Fourier transform to A_p, yielding

$$u_p(x,y) = F^{-1}\{A_p(\alpha,\beta)\} = J_x(x,y)+J_y(x,y) \quad \text{in} \quad \Omega_1 \tag{21}$$

$$u_p(x,y) = u_0 - F^{-1}\{\frac{\alpha^2+\beta^2-k_d^2}{\alpha^2+\beta^2-k_v^2}A_p(\alpha,\beta)\} = u_0 - I_x(x,y) - I_y(x,y) \quad \text{in} \quad \Omega_2 \tag{22}$$

Each term in (21) and (22) can be written as an integration over the complex angular spectrum plane. After singling out the contribution from the pole singularity, the integration can be written as, I_x for example,

$$I_x(x,y) = -H(2\pi-\phi_0,2\pi)R_x e^{-jk_v(x\cos\phi_0-y\sin\phi_0)} \tag{23}$$

$$-j/(4\pi)\int_{SDP} T_x\frac{-\sin w+\sqrt{\epsilon-\cos^2\phi_0}}{\cos w-\cos\phi_0}e^{-jk_v\rho\cos(w+\phi)}dw. \tag{24}$$

The first term in (24) in identified as the reflected wave due to the $x=0$ edge and is denoted as $-u_{g1}$. The other terms I_y, J_x, and J_y can be expressed in a similar way. Consequently, the total field can be written as the following summation:

$$u_p(x,y) = u_0(x,y)+\sum_{i=1}^{4}u_{gi}(x,y)+v_{1,2}(x,y) \tag{25}$$

where u_{g1} and u_{g2} are the reflected waves and u_{g3} and u_{g4} are the refracted waves. The v_1 and v_2 are diffracted waves in dielectric and free-space, respectively. They are given as steepest descent path (SDP) integrals

$$v_1(x,y) = j/(4\pi)\int_{SDP} f_1(w;\phi_0)e^{-jk_v\rho\cos(w-\phi)}dw \tag{26}$$

$$v_2(x,y) = -j/(4\pi)\int_{SDP} f_2(w;\phi_0)e^{-jk_d\rho\cos(w-\phi)}dw \tag{27}$$

where

$$f1(w;\phi_0) = T_x\frac{\sin w+\sqrt{\epsilon-\cos^2\phi_0}}{\cos w-\cos\phi_0}+T_y\frac{\cos w+\sqrt{\epsilon-\sin^2\phi_0}}{\sin w-\sin\phi_0} \tag{28}$$

$$f2(w;\phi_0) = T_x\frac{\sqrt{\epsilon}\sin w+\sqrt{\epsilon-\cos^2\phi_0}}{\sqrt{\epsilon}\cos w-\cos\phi_0}+T_y\frac{\sqrt{\epsilon}\cos w+\sqrt{\epsilon-\sin^2\phi_0}}{\sqrt{\epsilon}\sin w-\sin\phi_0} \tag{29}$$

One may realize that $f1$ and $f2$ have singularities at $\pi - \phi_0$, $2\pi - \phi_0$ and $\phi_1 = \cos^{-1}(\cos\phi_0/\sqrt{\epsilon})$, $\phi_2 = \sin^{-1}(\sin\phi_0/\sqrt{\epsilon})$, respectively. There four angles are exactly where the four optical boundaries (transition region) are located. For large ρ away from the transition regions, $v1$ and $v2$ can be evaluated asymptotically as

$$v_{1,2}(\rho,\phi) \simeq \pm 1/2 \frac{e^{-jk_{v,d}\rho - j\pi/4}}{\sqrt{2k_{v,d}\rho}} f_{1,2}(\phi;\phi_0) \tag{30}$$

The above analysis completes the PO solution of the scattering problem. However, one may refine the approximate solution by adding a correction term to A_P; that is

$$A_a(\alpha,\beta) = A_p(\alpha,\beta) + A_c(\alpha,\beta) \tag{31}$$

The actual field A_a satisfies the null-field condition in an exact way. This provides equations from which the correction field A_c can be solved. The equations are written in the spectral domain as

$$F^{-1}A_c(\alpha,\beta) = F^{-1}A_p(\alpha,\beta) = -v2 \quad \text{in} \quad \Omega_2 \tag{32}$$

$$F^{-1}\{\frac{\alpha^2+\beta^2-k_d^2}{\alpha^2+\beta^2-k_v^2}A_c(\alpha,\beta)\} = u_0 - F^{-1}\{\frac{\alpha^2+\beta^2-k_d^2}{\alpha^2+\beta^2-k_v^2}A_p(\alpha,\beta)\} = v1 \quad \text{in } \Omega_1 \tag{33}$$

Noting that $1/(\alpha^2+\beta^2-k_d^2)$ is the Fourier transform of the Green's function, one may introduce a virtual source function $S(\alpha,\beta)$ into (32) and (33) so that

$$F^{-1}\{\frac{S(\alpha,\beta)}{\alpha^2+\beta^2-k_d^2}\} = -v2 \qquad \text{in} \qquad \Omega_2 \tag{34}$$

$$F^{-1}\{\frac{S(\alpha,\beta)}{\alpha^2+\beta^2-k_v^2}\} = v1 \qquad \text{in} \qquad \Omega_1. \tag{35}$$

Hence, the diffracted field v_1 and v_2 can be viewed as the field produced by the virtual sources towards the dielectric and the free-space regions, respectively. It is reasonable to assume that the virtual source is located on the tip of the wedge and generates cylindrical waves outwards. Then the source may be represented by two-dimensional multipole series as

$$s(x,y) = \sum_{m=0}^{\infty}\sum_{n=0}^{\infty} a_{mn}\delta^{(m)}(x)\delta^{(n)}(y) \tag{36}$$

Since v_1 and v_2 are analytical within Ω_1 and Ω_2 respectively, they can be used to determine the multipole expansion coefficients. Substitution of (36) into (34) and (35) gives a dual series equation for a_{mn}:

$$\sum_{m,n} a_{mn}(-jk_v\cos w)^m(-jk_v\sin w)^n = f_1(w;\phi_0) \qquad \text{in}\Omega_1 \tag{37}$$

$$\sum_{m,n} a_{mn}(-jk_d\cos w)^m(-jk_d\sin w)^n = f_2(w;\phi_0) \qquad \text{in}\Omega_2 \tag{38}$$

After a_{mn} is solved numerically form the above equation, the correction diffracted field pattern $g1(w;\phi_0)$ and $g2(w;\phi_0)$ can be constructed from (34) and (35) for the entire space. Then they are added to the PO diffracted field pattern $f_1(w;\phi_0)$ and $f_2(w;\phi_0)$ to obtain the corrected field pattern which are used in (30) instead of $f_1(w;\phi_0)$ and $f_2(w;\phi_0)$ to calculate the corrected far field. The corrected field still has singularity on the optical boundaries. On those transition regions, one need to use Fresnel integrals to obtain a uniformly valid result, as indicated in [3].

In order to have a better understanding of the method, a computer code is written to implement the PO solution and the numerical correction. Figure 2 shows the total field amplitude around a dielectric wedge with symmetrical plane wave incidence ($\phi_0 = 180^o$). The observation point is fixed at $\rho = 2\lambda$ away from the origin and the observation angle ϕ varies from 0^o to 360^o. The dielectric wedge has a apex angle of $\pi/2$ and a relative permittivity of $\epsilon_r = 2.0$. The dashed line denotes the solution before numerical correction and the solid line denotes the solution after numerical correction. It is observed that the correction is most significant inside the dielectric region, where the two refraction boundaries are close to each other. The corrected formulation assures the vanishing of the diffracted field on the dielectric interface ($\phi = 0^o$ and $\phi = 90^o$), thus guarantees that the continuity condition on the dielectric interface is satisfied, as can be observed in Fig. 2. Figure 3 shows the total field amplitude around the same dielectric wedge with the observation point fixed to be $\rho = 5\lambda$ away from the origin. As one may expect, more rapid field amplitude variation is observed in Fig. 3. There is a peak in the field amplitude inside the dielectric wedge, as the result of interference of two refracted waves.

The method can be extended to dielectric wedge with arbitrary angle [7], [8]. However, the choice of right angle helps to simplify the problem by reducing the PO fields into four distinct terms. For an arbitrary-angled wedge problem, multiple reflection and refraction may occur and the resultant PO fields are generally not only four terms. However, the extension to wedges with arbitrary angles are straightforward, given the framework of [3]. Apart from theoretical formulations, there are still numerical issues regarding the solving of the monopole coefficients. For a dielectric wedge with large dielectric constant, one needs to add more expansion terms to model the abrupt change from free-space to dielectric. However, the linear system of equations represented by (37) and (38) are typically ill-conditioned. This is even worse when one tries to keep more expansion terms in the infinite summation. This implies that, without special treatment, the proposed method may become less accurate for dielectric wedge with large refractive index.

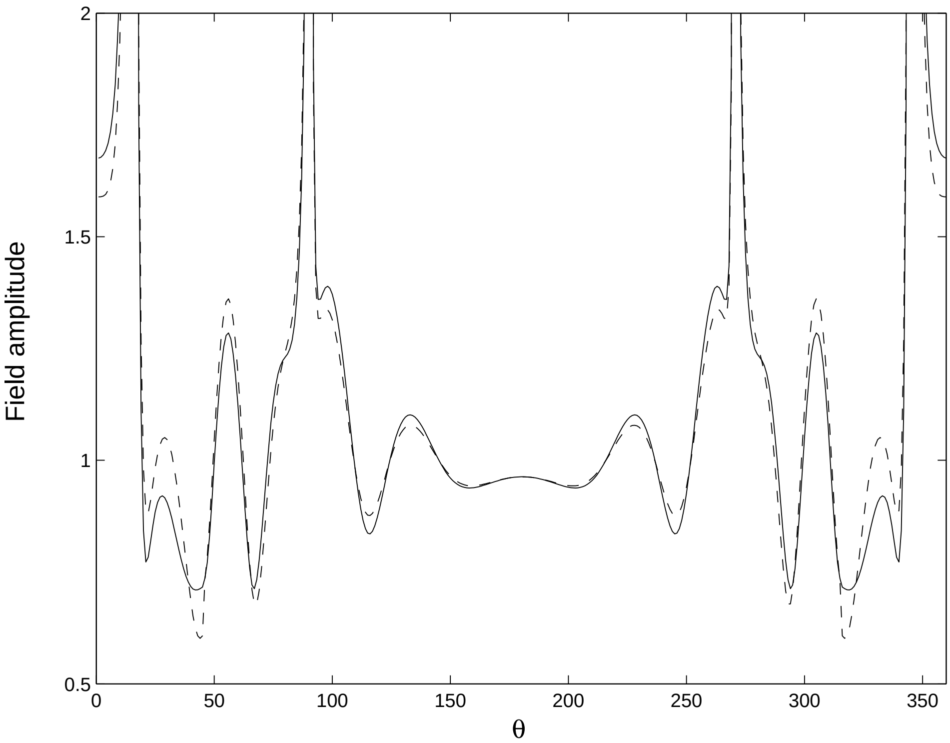

Figure 2: Field amplitude for the right angle dielectric wedge. $\rho = 2\lambda$

6 Integral-Transform Method - Isorefractive Wedge

An isorefractive wedge is a dielectric wedge whose isotropic material has a refractive index equal to that of the surrounding medium. Or more specifically, $\epsilon_r \mu_r = 1.0$. This implies that the wavenumbers are identical inside and outside the wedge. Mathematically, this simplified the analysis significantly since the radial wavefunctions have the same argument inside and outside the wedge, making possible one-to-one mode matching of the field expansions. Exact solutions to this particular case are available. In the work represented by [4] and [5], an integral-transform method is employed to obtain a uniform and exact solution.

From Maxwell's equations and Green's theorem, one may arrive at integral equations regarding the total field which are given by

$$u_i^S(R) - \kappa u^S(R) = \eta \int_{0+}^{\infty} L(R, r) u^S(r) dr \tag{39}$$

$$u_i^A(R) - \kappa u^A(R) = -\eta \int_{0+}^{\infty} L(R, r) u^A(r) dr \tag{40}$$

where $\eta = 1 - \epsilon$ and $\kappa = 1 - \eta/2$. The superscripts S and A denote symmetric and antisymmetric components of the total field, respectively. The integral

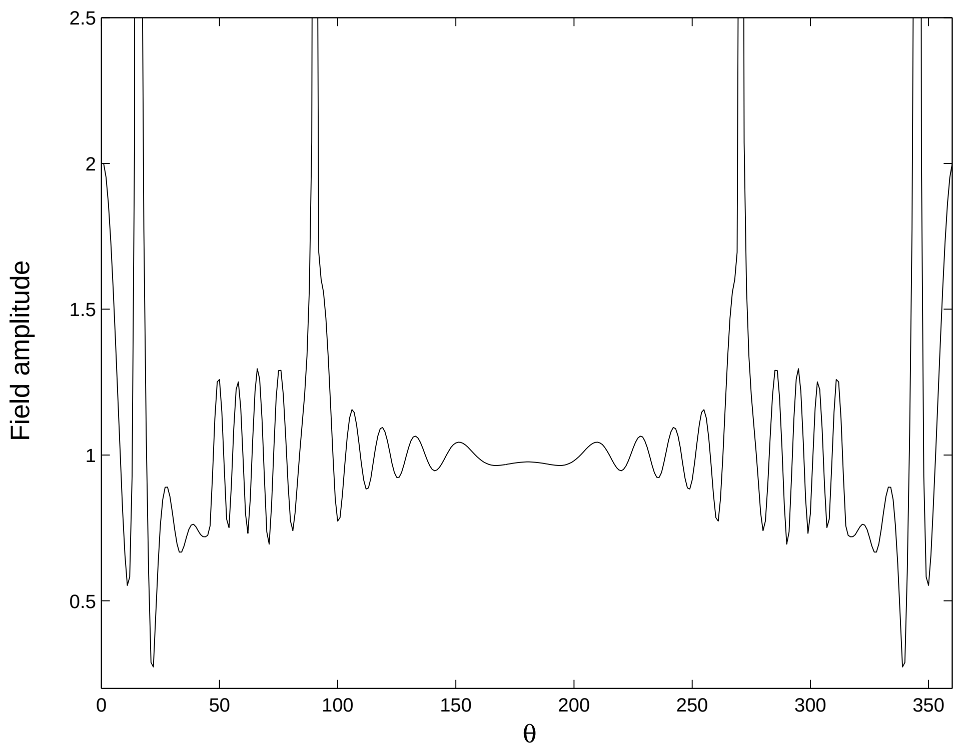

Figure 3: Field amplitude for the right angle dielectric wedge. $\rho = 5\lambda$

kernel L is given by

$$L(R,r) = \frac{-jk}{4} R\sin(2\chi)\frac{H_1^{(2)}(k\sqrt{R^2+r^2-2rR\cos(2\chi)})}{\sqrt{R^2+r^2-2rR\cos(2\chi)}}. \tag{41}$$

In order to solve (41) analytically, the Kantorovich-Lebedev transform is used. The transform pair is given by

$$\tilde{u}(\nu) = \int_0^\infty u(r)H_\nu^{(2)}(kr)r^{-1}dr \tag{42}$$

$$\tilde{u}(r) = -1/2\int_{-j\infty}^{j\infty} \nu J_\nu(kr)\tilde{u}(\nu)d\nu \tag{43}$$

Also, from an integral equation formulation of Gegenbauer's addition theorem one may rewrite $L(R,r)$ as

$$L(R,r) = 1/r\int_0^{j\infty} \psi(\nu, 2\chi)H_\nu^{(2)}(kR)H_\nu^{(2)}(kr)d\nu \tag{44}$$

where

$$\psi(\nu,\Omega) = \frac{-j}{4}\nu e^{-j\pi\nu}\sin(\nu(\pi-\Omega)). \tag{45}$$

Using the inverse Kantorovich-Lebedev transform (43) and (44), the integral equations (39) and (40) can be written as

$$\begin{aligned}&\int_0^{j\infty} H_\nu^{(2)}(kR)\rho(\nu)[\tilde{u}_i(\nu) - \kappa\tilde{u}(\nu)]d\nu \\ = \quad &\pm\eta \int_0^{j\infty} H_\nu^{(2)}(kR)\psi(\nu, 2\chi)\tilde{u}(\nu)d\nu \end{aligned} \tag{46}$$

where $\rho(\nu) = \nu(e^{-2j\pi\nu} - 1)/4$. Since $H_\nu^{(2)}(kR)$ are independent functions, the above equality requires that

$$\rho(\nu)[\tilde{u}_i(\nu) - \kappa\tilde{u}(\nu)] = \psi(\nu, 2\chi)\tilde{u}(\nu). \tag{47}$$

This equation relates the total field to the incident field in the Kantorovich-Lebedev domain. Applying the inverse Kantorovich-Lebedev transform, one is able to find the total field $u(x, y)$ in the spacial domain. The final result for a plane wave incident upon an isorefractive wedge is provided by the authors and turns out to be represented by a series of Bessel functions [4]. The field inside the wedge, for example, is given by

$$u^S(\rho, \phi) = 2\pi(\Lambda + 1)\sum_{0+}^{\infty} J_{s_n}(k\rho)e^{-j\pi s_n/2}\cos(s_n\phi)\cos[s_n(\pi - \phi_0)]\Xi^S(s_n) \tag{48}$$

$$u^A(\rho, \phi) = -2\pi(\Lambda+1)\sum_{1}^{\infty} J_{a_n}(k\rho)e^{-j\pi a_n/2}\cos(a_n\phi)\cos[a_n(\pi-\phi_0)]\Xi^S(a_n) \tag{49}$$

where $\Lambda = (1 - \epsilon)/(1 + \epsilon)$ and

$$\Xi^{S,A}(\nu) = \frac{1}{\pi\cos(\nu\pi) \pm \Lambda(\pi - \Omega)\cos[\nu(\pi - \Omega)]} \tag{50}$$

The s_n and a_n are Greenburg poles (symmetric and antisymmetric pole, respectively). When $\chi = \pi/2$ where the dielectric wedge becomes an infinite plane, or when $\epsilon = 1.0$, the Greenburg poles take integer values. Therefore the total field is represented by a series of bessel functions of integer order, as indicated by the plane-wave-to-cylindrical-wave transform (15). For an isorefractive wedge with arbitrary χ and ϵ, the Greenburg poles generally contain both integer and fractional values. All Greenburg poles contribute to the solution of the problem, but only the smallest ones (s_1 and a_1) induce field singularity [4].

A computer code is written to implement the global field solution given by [4], as a demonstration of the proposed method. The contour plot for the field amplitude is shown in Fig. 4 for $\phi_0 = 180^o$ (symmetrically incidence) and Fig. 5 for $\phi_0 = -90^o$. In both cases, the dielectric wedge has an angle of $\pi/2$ and relative permittivity $\epsilon_r = 2.0$. The contributions from individual series terms are also plotted (not shown in the report) and reveal decaying magnitude and increasing spacial variation with larger term index.

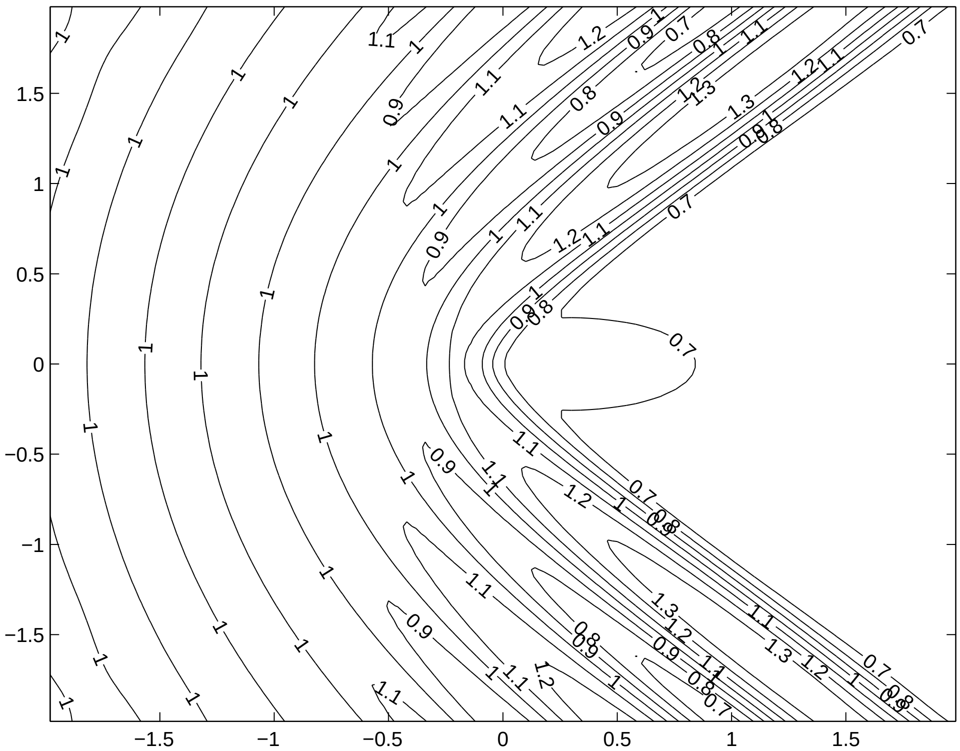

Figure 4: Contour plot of the field amplitude. $\phi_0 = 0^o$

7 Conclusion

This report reviews several papers on the analytical analysis of diffraction by a dielectric wedge. While a complete solution of the problems is not found in literature, approximate results are provided and extension to numerical methods are made. In the modal analysis [1], fields inside and outside the dielectric wedge is expanded with bessel functions and boundary condition is matched for different modes. The mode matching process is facilitated by a formula that relates the bessel functions of different arguments. The expansion coefficients are then solved iteratively from a coupled series-equation. In the work by Yeo *et al.* [2], the entire spacial domain is divided into several sectors by the optical boundaries, and bessel functions are used to expand the field within each sector. The expansion coefficients are determined from the continuity conditions on the optical boundaries. Joo *et al.* formulate a hybrid method that combines the PO solution with a numerical improvement [3]. First an integral equation is solved in the spectral domain. Then the total field is obtained by applying the inverse Fourier transform, which results in an integration over the complex angular spectrum domain. The singularity contribution to the integration is separated and turns out to be the reflected (or refracted) fields. The rest of the integration contributes to the diffracted field. A more rigorous solution can be obtained by adding a correction field to the PO field. A spectral-domain equation is derived for the correction field and it

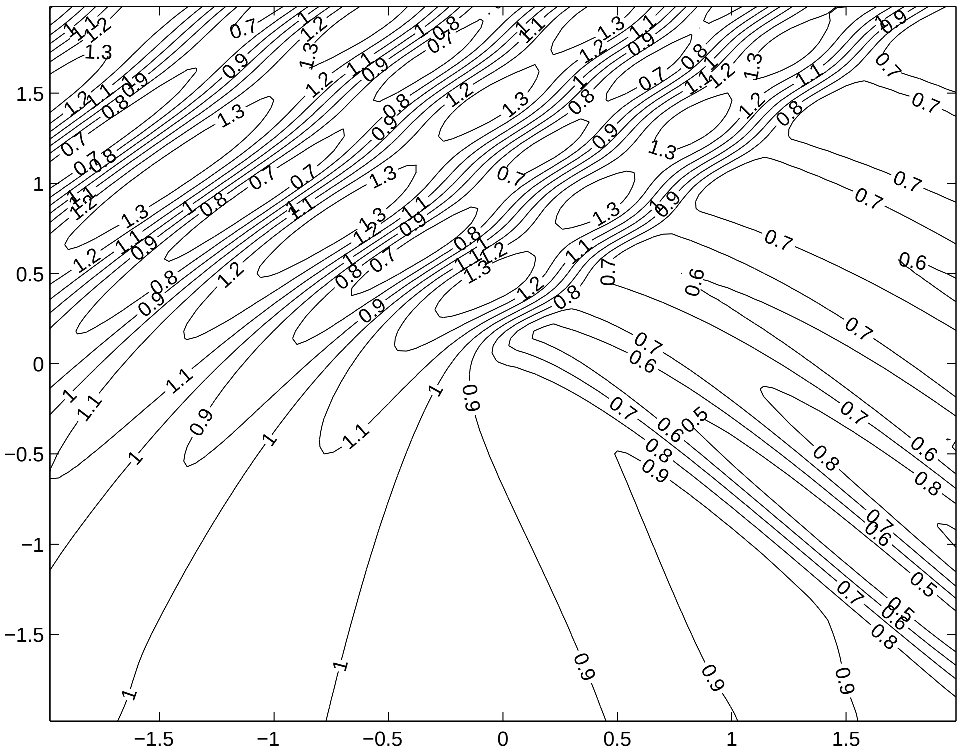

Figure 5: Contour plot of the field amplitude. $\phi_0 = -90^o$

is shown that the correction fields are equivalently cylindrical waves radiated by multipole sources located on the tip of the wedge. The multipole expansion coefficients are solve numerically and the correction field can be recovered accordingly. Finally, a relatively new paper [4] is reviewed on the scattering by isorefractive wedges. For this special type of dielectric wedge, exact analytical solution can be obtained via the Kantorovich-Lebedev transform. According to the paper, a uniform solution can be obtained for the entire space, expressed as a summation of bessel functions whose order are determined by Greenburg poles.

Through these analytical methods, better knowledge is gained for the reflection, refraction, and diffraction by a dielectric wedge, especially the field behavior near the apex of the wedge. New features, such as the interference of refracted waves inside the wedge, are exhibited, which are not observed in the case of conducting wedges. These analytical or combined analytical-numerical solutions are also valuable in providing reliable references for a comprehensive numerical analysis.

References

[1] R. H. T. Bates, “Wavefunctions for prisms,” *Int. J. Electronics.*, vol. 34, No. 1, pp. 81-95, 1973.

[2] T. S. Yeo, D. J. N. Wall, and R. H. T. Bates "Diffraction by a prism," *J. Opt. Soc. Am. A*, vol. 2, No. 6, pp. 964-969, June 1985.

[3] C.-S. Joo, J.-W. Ra, and S.-Y. Shin, "Scattering by right angle dielectric wedge," *IEEE Trans. Antennas Propagat.*, vol. 32, No. 1, pp. 61-69, Jan. 1984.

[4] L. Knockaert, F. Olyslager, and D. D. Zutter, "The diaphanous wedge," *IEEE Trans. Antennas Propagat.*, vol. 45, No. 9, pp. 1374-1381, Sept. 1997.

[5] P. L. E. Uslenghi, "Exact scattering by isorefractive bodies," *IEEE Trans. Antennas Propagat.*, vol. 45, No. 9, pp. 1382-1385, Sept. 1997.

[6] G. James, *Geometrical Theory of Diffraction for Electromagnetic Waves*, 3rd Edition, The Institution of Electrical Engineers, 1986.

[7] S.-Y. Kim, J.-W. Ra, and S.-Y. Shin, "Diffraction by an arbitrary-angled-dielectric wedge: Part I – physical optics approximation," *IEEE Trans. Antennas Propagat.*, vol. 39, No. 9, pp. 1272-1281, Sept. 1991.

[8] S.-Y. Kim, J.-W. Ra, and S.-Y. Shin, "Diffraction by an arbitrary-angled-dielectric wedge: Part II – correction to physical optics solution," *IEEE Trans. Antennas Propagat.*, vol. 39, No. 9, pp. 1282-1292, Sept. 1991.